Optically anisotropic infinite cylinder above an optically anisotropic half space: Dispersion interaction of a single-walled carbon nanotube with a substrate

A. Šiber
Institute of Physics, Bijenička cesta 46, P.O. Box 304, 10001 Zagreb, Croatia

R. F. Rajter
Department of Materials Science and Engineering, Massachusetts Institute of Technology, 77 Massachusetts Avenue, Cambridge, Massachusetts 02139

R. H. French
DuPont Co. Central Research, Experimental Station E400-5207, Wilmington, Delaware 19880

W. Y. Ching
Department of Physics, University of Missouri-Kansas City, Kansas City, Missouri 64110

V. A. Parsegian
Department of Physics, University of Massachusetts, Amherst, Massachusetts 01003

R. Podgornik[a)]
Laboratory of Physical and Structural Biology, NICHD, National Institutes of Health, Building 9, Bethesda, Maryland 20892-0924, Department of Physics, Faculty of Mathematics and Physics and Institute of Biophysics, School of Medicine, University of Ljubljana, SI-1000 Ljubljana, Slovenia, and Department of Theoretical Physics, J. Stefan Institute, SI-1000 Ljubljana, Slovenia

A complete form of the van der Waals dispersion interaction between an infinitely long anisotropic semiconducting/insulating thin cylinder and an anisotropic half space is derived for all separations between the cylinder and the half space. The derivation proceeds from the theory of dispersion interactions between two anisotropic infinite half spaces as formulated in Phys. Rev. A **71**, 042102 (2005). The approach is valid in the retarded as well as nonretarded regimes of the interaction and is coupled with the recently evaluated *ab initio* dielectric response functions of various semiconducting/insulating single wall carbon nanotubes, enables the authors to evaluate the strength of the van der Waals dispersion interaction for all orientation angles and separations between a thin cylindrical nanotube and the half space. The possibility of repulsive and/or nonmonotonic dispersion interactions is examined in detail. © *2010 American Vacuum Society.* [DOI: 10.1116/1.3416904]

I. INTRODUCTION

Single walled carbon nanotubes (SWCNTs) are unique materials with chirality-dependent dielectric properties[1] that make a clear imprint on their van der Waals-dispersion interactions.[2,3] Several experimental procedures have been proposed to exploit the differences between these properties in order to separate SWCNTs by chirality (see Ref. 3 and references therein). Different separation mechanisms have been suggested and tested[4] but we are still some way off to separate a nanotube mixture into its single chirality components. Nevertheless, techniques such as size-exclusion chromatography (SEC) coupled to decorating the SWCNTs with ss-DNA seem very promising. In order to understand the interaction of a SWCNT with a substrate in the context of SEC the details of the van der Waals dispersion (vdW) interactions are quite relevant and their details need to be sorted out.

SWCNT materials consist of bundles of aligned carbon nanotubes that can contain large number of carbon nanotubes[5] so that the bundle itself can be considered as a bulk material with anisotropic dielectric properties and a large exposed surface. In the bundle the SWCNTs are kept together by attractive vdW interactions. One may be interested to compute the energy needed to separate one of the tubes from the rest of the bundle, depending on the tube's position in the bundle. We are thus led back again to the problem of vdW interactions between a single SWCNT and a substrate.

For all such and similar applications a knowledge of vdW interactions between materials of anisotropic dielectric properties is thus a requisite. The vdW interactions between two semiconducting/insulating thin cylinders have already been examined in the nonretarded[2] and retarded[6] regimes, and as the next logical step, in this article we examine the vdW forces between an optically anisotropic infinite cylinder and an optically anisotropic half-space substrate. Our approach does not consider finite-size effects, i.e., the cylinder that we examine is always infinitely long and infinitely thin. Infinitely thin in this context means that the thickness of the cylinder is the smallest length scale in the system. This effectively sets the range of applicability of our method for the

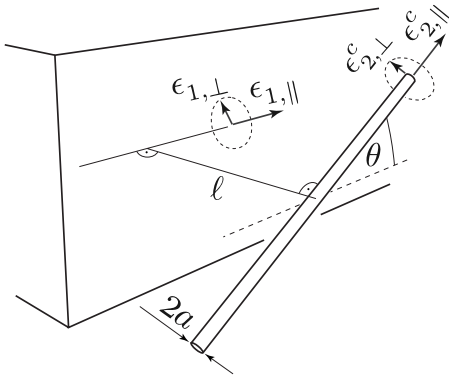---

a)Electronic mail: podgornr@mail.nih.gov

FIG. 1. Illustration of the system of interest to us with some of the quantities required in the derivation of dispersion interaction.

evaluation of vdW interactions.[6] For separations between the cylinder and the substrate on the order or less than the thickness of the cylinder, a different approach is in order and has indeed been derived elsewhere.[2]

In what follows the axis of the thin cylinder is assumed to be always parallel to the half-space surface. The principal optical axes of the half space and the cylinder may however be nonparallel, making an angle that we denote by θ. The coordinate system is oriented so that the dielectric tensor of the half space is diagonal. The transverse responses are isotropic in the plane perpendicular to the longitudinal axis, both for the cylinder and in the half space. The system that we consider is sketched in Fig. 1. It is our aim to derive closed-form expressions for the vdW dispersion interaction energy in such a system, accounting for the effects of retardation exactly, which shall enable us to estimate their importance.

II. DERIVATION OF THE FORMULAS FOR DISPERSION INTERACTION

In what follows we will calculate the vdW interaction between an extended cylindrical object and a semi-infinite slab of a dielectric material. The vdW interaction is of course nothing but the Casimir interaction evaluated for realistic, i.e., nonmetallic boundary conditions at a finite value of the temperature.[7,8] The theory of vdW interactions between two semi-infinite half spaces was set fourth in all its detail by Lifshitz in 1955.[7,8] From the interaction free energy between two half spaces one can extract the interaction between a cylinder and one semi-infinite half space by assuming that the other half space is a dilute assembly of anisotropic cylinders. The derivation closely follows the arguments of Pitaevskii[9] for evaluating the vdW interactions between isotropic impurity atoms in a homogeneous fluid and has been used by us previously in the evaluation of the vdW interactions between two cylinders.[6]

The Pitaevskii approach to vdW interactions between two small objects or a small object and a half space works only if the object, i.e., the cylinder in this case, has a sufficiently small radius, a, which must be the smallest length scale entering the problem. In this case the single scattering approxi-

mation, which is what the Pitaevskii approach amounts to if compared to the exact general formulation,[10] gives the lowest order contribution in terms of the cylinder radius. Furthermore, its dielectric response should be finite for all Matsubara frequencies including zero, and thus should most notably not contain the Drude peak at zero frequency as presented in idealized metals.[6] Metallic cylinders are thus excluded from our consideration. With the above two provisos our approach yields the lowest order single scattering approximation to the vdW interactions between a cylinder and an anisotropic dielectric half space, if compared to the exact general multiple scattering formulation.[10]

As in Ref. 6, we start the derivation of the vdW interactions between an optically anisotropic cylinder and a planar substrate from the expression for dispersion interaction between two anisotropic half spaces derived by Barash and co-workers.[11] The two half spaces ["left" (1) and "right" (2)] are separated by ℓ and their principal optical axes are parallel to the surface planes of the two half spaces but rotated with respect to each other by angle θ. For our purposes, we consider the right half space (2) to be composed of aligned cylinders of radii a at volume fraction v, with $\epsilon_{2,\perp}^c$ and $\epsilon_{2,\|}^c$ as the transverse and longitudinal dielectric response functions of the cylinder materials [note that here we separate the notion of material the cylinder is made of (quantities denoted by superscript c) from the material that the cylinders make, i.e., we separately consider the dielectric response of an *individual* cylinder from the response of the material made of cylinders—the two concepts can be easily related as demonstrated in Ref. 7]. We treat the left (1) half space as an anisotropic continuous medium with $\epsilon_{1,\perp}$ and $\epsilon_{1,\|}$ as its transverse and longitudinal dielectric responses. We can formally "rarify" the right medium using a well defined mathematical procedure (see Refs. 7 and 6) that yields the interaction between an individual cylinder and the left half space [$g(\ell, \theta)$].

We can write the dielectric response of the right half space as a function of the dielectric responses of individual cylinders (assuming local hexagonal packing symmetry, see Ref. 7, p. 318) as

$$\epsilon_{2,\|} = \epsilon_3(1 + v\Delta_\|),$$

$$\epsilon_{2,\perp} = \epsilon_3\left(1 + \frac{2v\Delta_\perp}{1 - v\Delta_\perp}\right), \tag{1}$$

where ϵ_3 is the dielectric response of the isotropic medium that the cylinder is immersed in (and that permeates the space between the cylinders in the right half space as we formally rarify it). The relative anisotropy measures of the cylinder are given by

$$\Delta_\perp = \frac{\epsilon_{2,\perp}^c - \epsilon_3}{\epsilon_{2,\perp}^c + \epsilon_3}, \quad \Delta_\| = \frac{\epsilon_{2,\|}^c - \epsilon_3}{\epsilon_3}. \tag{2}$$

Using these substitutions, the dispersion interaction between the two half spaces becomes a function of the volume fraction, v.

To obtain the interaction free energy per unit length of the cylinder, $g(\ell, \theta)$, between a single cylinder and a half-space

substrate, one takes the interaction free energy per unit surface area between two half spaces, $G(\ell, \theta, v)$, and expands it to the first order in v. It then follows that[7]

$$Ng(\ell, \theta) = -\frac{\partial G(\ell, \theta, v)}{\partial \ell}, \tag{3}$$

where $G(\ell, \theta, v)$ is given by Barash's interaction formula[11] rewritten so as to account for the fact that the right half space is made of aligned cylinders at volume fraction v. The distance between the cylinder and the substrate is denoted by ℓ,

and $N = v/(\pi a^2)$ (see Fig. 1). One then Taylor expands $G(\ell, \theta, v)$ with respect to v and differentiates the first order term with respect to ℓ, obtaining a quantity proportional to $g(\ell, \theta)$, as can be seen from Eq. (3). This procedure yields a result that is fairly complicated,

$$g(\ell, \theta) = \frac{k_B T a^2}{4\pi} \sum_{n=0}^{\infty} {}' \int_0^\infty Q dQ \int_0^{2\pi} d\phi \left[e^{-2\ell\rho_3} \frac{\mathcal{N}}{\mathcal{D}} \right], \tag{4}$$

where

$$\mathcal{N} = \left(\frac{\Delta_\|}{2} - \Delta_\perp\right)\{Q^2 \sin^2(\phi + \theta) \times [\widetilde{f}(\phi)\epsilon_{1,\perp}(Q^2 \sin^2 \phi(\rho_{1,\perp} + \rho_3) + \rho_{1,\perp}\rho_3(\rho_3 - \rho_{1,\perp})) + (\epsilon_{1,\perp} - \epsilon_3)(\rho_3(\rho_{1,\perp} + 2\rho_3) - Q^2)]$$

$$- 2\widetilde{f}(\phi)\epsilon_{1,\perp}\rho_{1,\perp}\rho_3^2[2Q^2 \sin \phi \cos \theta \sin(\phi + \theta) + \rho_3^2 \sin^2 \theta] + \widetilde{f}(\phi)\epsilon_{1,\perp}\rho_3^2[Q^2 \sin^2 \phi(\rho_{1,\perp} - \rho_3) + \rho_{1,\perp}\rho_3(\rho_{1,\perp} + \rho_3)]$$

$$+ \rho_3^3(\epsilon_3 - \epsilon_{1,\perp})(Q^2 + \rho_{1,\perp}\rho_3)\} + 2\widetilde{f}(\phi)\Delta_\perp\epsilon_{1,\perp}[Q^2 \sin^2 \phi(Q^2\rho_{1,\perp} - \rho_3^3) + \rho_{1,\perp}\rho_3^2(Q^2 \cos(2\phi) + \rho_{1,\perp}\rho_3)] - \Delta_\perp(\epsilon_{1,\perp} - \epsilon_3)$$

$$\times[(Q^2 + \rho_3^2)(Q^2 + \rho_{1,\perp}\rho_3) + (Q^2 - \rho_3^2)(Q^2 - \rho_{1,\perp}\rho_3)] \tag{5}$$

and

$$\mathcal{D} = \rho_3(\rho_{1,\perp} + \rho_3)\{\epsilon_{1,\perp}\widetilde{f}(\phi)[Q^2 \sin^2 \phi - \rho_{1,\perp}\rho_3] + \epsilon_{1,\perp}\rho_3 + \epsilon_3\rho_{1,\perp}\}. \tag{6}$$

In the equations above,

$$\rho_{1,\perp} = \sqrt{Q^2 + \frac{\epsilon_{1,\perp}\omega_n^2}{c^2}},$$

$$\rho_3 = \sqrt{Q^2 + \frac{\epsilon_3\omega_n^2}{c^2}},$$

$$\widetilde{f}(\phi) = \frac{\sqrt{Q^2((\epsilon_{1,\|}/\epsilon_{1,\perp}) - 1)\cos^2 \phi + \rho_{1,\|}^2} - \rho_{1,\perp}}{Q^2 \sin^2 \phi - \rho_{1,\perp}^2}, \tag{7}$$

and c is the speed of light. Subscript n indexes the (thermal) Matsubara frequencies and the prime on the summation means that the weight of the $n=0$ term is 1/2 (see Refs. 7 and 13 for details). All the dielectric responses should be considered as functions of discrete imaginary Matsubara frequencies, i.e., as $\epsilon_3 \equiv \epsilon_3^{(n)} = \epsilon_3(i\omega_n)$, $\Delta_\perp(i\omega_n)$ and $\Delta_\|(i\omega_n)$, and $\epsilon_{1,\perp}(i\omega_n)$ and $\epsilon_{1,\|}(i\omega_n)$. The frequencies in the Matsubara summation are $\omega_n = 2n\pi k_B T/\hbar$.

We have not been able to simplify the expressions further using the routines from MATHEMATICA.[14] However, we did examine the nonretarded limit of the expressions we derived. In particular, we have performed the same analytical procedure as specified above, only instead of $G(\ell, \theta, v)$, we have taken $\lim_{c\to\infty} G(\ell, \theta, v)$. We obtained

$$g(\ell, \theta) = \frac{k_B T a^2}{16\pi\ell^3} \sum_{n=0}^{\infty} {}' \mathcal{F}_n(\theta, \phi), \tag{8}$$

where

$$\mathcal{F}_n(\theta, \phi) = 2 \int_0^{2\pi} d\phi \Delta_{\mathcal{L}m}(\phi) \left[\Delta_\perp + \frac{1}{4}(\Delta_\| - 2\Delta_\perp)\cos^2(\phi + \theta) \right] \tag{9}$$

and

$$\Delta_{\mathcal{L}m}(\phi) \equiv \frac{\epsilon_3 - \epsilon_{1,\perp}\sqrt{(\epsilon_{1,\|} - \epsilon_{1,\perp})\cos^2(\phi) + \epsilon_{1,\perp}/\epsilon_{1,\perp}}}{\epsilon_3 + \epsilon_{1,\perp}\sqrt{(\epsilon_{1,\|} - \epsilon_{1,\perp})\cos^2(\phi) + \epsilon_{1,\perp}/\epsilon_{1,\perp}}}. \tag{10}$$

One can easily check that the nonretarded limit of our result is the *same* as Eq. (17) of Ref. 2, up to the sign of θ, which is irrelevant (the result is symmetric with respect to $\theta \to -\theta$).

III. NUMERICAL RESULTS FOR THE DISPERSION INTERACTION

Although the analytical result for the retarded dispersion interaction is quite complicated it can be easily evaluated numerically. As in Ref. 6, we shall concentrate on single wall carbon nanotubes as the prototype anisotropic cylinders. We obtain their spectral properties from the *ab initio* numerical methods in the optical range, as detailed in Ref. 2. We first construct the left half space by using a kind of inversion of the "rarification" procedure, i.e., we construct its response from the response of individual cylinders that are hexagonally arranged and perfectly aligned in the half space. The arrangement and geometry of cylinders are illustrated in Fig.
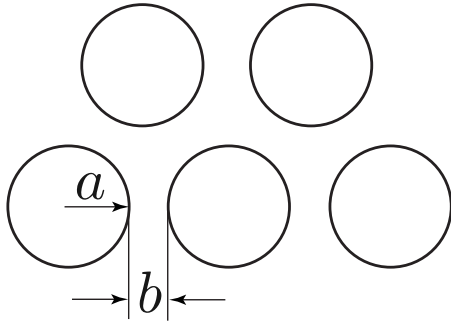
FIG. 2. Arrangement of cylinders and specification of distances used to construct the dielectric response of the left half space.
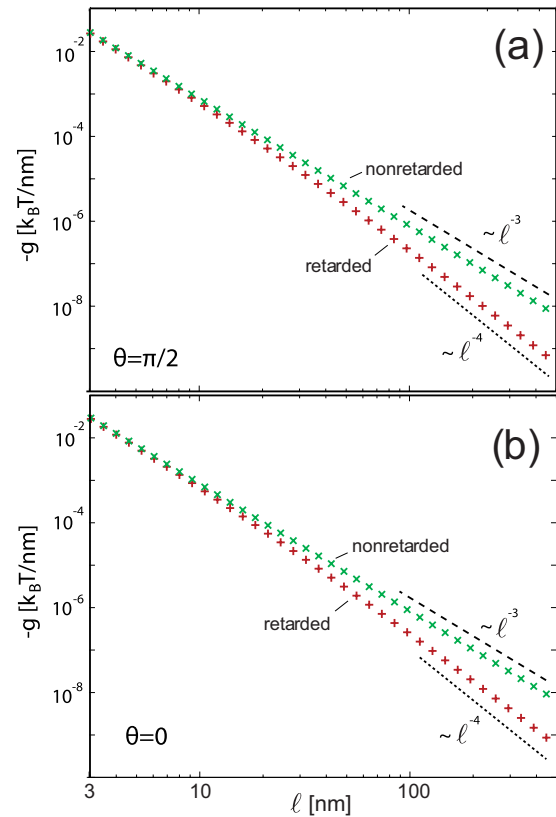

FIG. 3. (Color online) vdW interaction for a (6,5) carbon nanotube above a half space made of (6,5) carbon nanotubes as a function of distance (ϵ_3 =1) for $\theta = \pi/2$ (panel a) and $\theta = 0$ (panel b). The values of dispersion interaction with retardation included are indicated by (red) pluses. The nonretarded values are indicated by (green) ×'s. The power-law behaviors ℓ^{-4} and ℓ^{-3} are denoted by dotted and dashed lines, respectively.

2 (this should be thought of as the cross section of the half space in the plane of transverse response).

The dielectric response of such a material can be constructed from Eq. (1) presuming one sets in the appropriate v, which can be easily calculated from geometry. It is easy to see that

$$v = \frac{2\pi a^2}{(2a+b)^2 \sqrt{3}} = \frac{2\pi}{\sqrt{3}(2+(b/a))}. \quad (11)$$

Note that v is by construction always smaller than 1, even when $b=0$, which is as it should be. Since we are interested in carbon nanotubes, we take $b=0.34$ nm, which is the distance between graphene planes in graphite. This gives v =0.43 for $a=0.373$ nm, which is the radius of (6,5) carbon nanotubes.[2] The (6,5) carbon nanotubes are semiconducting and therefore appropriate for the illustration of the method we developed. We are now in a position to evaluate the interaction between a (6,5) carbon nanotube and a half space made of hexagonally arranged (6,5) carbon nanotubes. The half space can be thought of as an infinite bundle of SWCNTs. Our results are contained in Fig. 3. The calculations were performed for $\theta = \pi/2$, i.e., when the longitudinal axes of the cylinder and the half space are mutually perpendicular (panel a), and for $\theta = 0$, i.e., when the longitudinal axes of the two subsystems are parallel (panel b). The medium permeating the space around the cylinder is vacuum, so $\epsilon_3(i\omega) = 1$, $\forall \omega$.

We should add here that for illustrative purposes we disregarded the finite wall thickness of the (6,5) SWCNT and approximated it as if filled completely with the dielectric material. Taking into account the finite thickness of the wall would require a more careful modeling of its effective dielectric response[3] and thus introduce additional parameters that would complicate the understanding of the retardation effects in van der Waals—dispersion interactions between this SWCNT and the half space, which is our primary aim in this article. Also, once the surface-to-surface separation between a SWCNT and the half space is greater than approximately two SWCNT outer diameters,[3] this approximation turns out to work quite well. In the case the (6,5) SWCNT, this would mean greater than 1.5 nm. We thus excluded separations below 2 nm from all the graphs. At separations less than about 2 nm one would also need to derive the small

separation limit of the interaction free energy, which we do not consider here (for two interacting SWCNTs it was considered in Ref. 2).

Let us first estimate the importance of retardation effect for distances comparable to the radius of the (6,5) carbon nanotubes. For $\ell = 4$ nm, retarded value of the dispersion interaction is $-0.011\,52$ $k_B T/$nm, while the nonretarded value is $-0.012\,44$ $k_B T/$nm ($\theta = \pi/2$). This means that the contribution of retardation at this distance is about 7%. Interestingly, the contribution of retardation is about three times larger than was the case in cylinder-cylinder interaction studied in Ref. 6. One can visually detect differences in the functional behavior of retarded and nonretarded interactions already at $\ell = 10$ nm. When $\ell > 100$ nm, the ℓ^{-4} dependence of the retarded interaction becomes clearly visible, while the nonretarded interaction is proportional to the inverse third power of the separation for all separations, as can also be seen in Eq. (8). One can obtain the ℓ^{-4} dependence of the retarded interaction for large separation using the scaling arguments as follows. We use dimensionless combination of variables
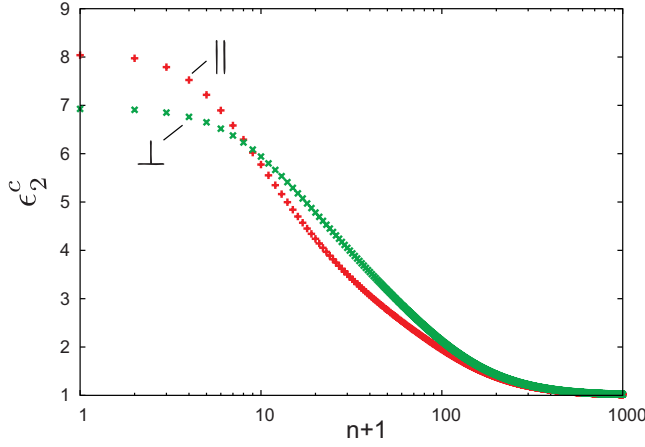
$$Q \equiv \frac{u}{\ell},$$

FIG. 4. (Color online) Dielectric responses (along imaginary axis) of the (6,5) SWCNT. The (red) pluses and (green) ×'s show the longitudinal and transverse responses, respectively. On the *x*-axis is the (shifted) Matsubara frequency index.

$$p \equiv \frac{\omega_n}{c}\ell. \tag{12}$$

This substitution is particularly efficient in the $T \to 0$ limit when the summation over n can be converted into an integration over a continuous variable p. We have

$$\sum_n \to \frac{\hbar}{2\pi k_B T} \frac{c}{\ell} \int dp,$$

$$\int Q dQ \to \frac{1}{\ell^2} \int u du. \tag{13}$$

Examining now the $\mathcal{N}/\mathcal{D}$ ratio in Eq. (4) we see that it is proportional to Q times some complicated dimensionless function containing dielectric responses and angles. Gathering all the dimensionalization constants together we have that

$$\lim_{T \to 0} g(\ell, \theta) = \frac{\hbar a^2 c}{8\pi^2 \ell^4} \bar{g}(\epsilon_3(0), \Delta_\parallel(0), \Delta_\perp(0), \epsilon_{1,\parallel}(0), \epsilon_{1,\perp}(0), \theta), \tag{14}$$

where in the $T \to 0$ limit, only the static dielectric response remains. We see that in this limit the interaction scales with inverse fourth power of separation (ℓ^{-4}).

One notes that the differences in interaction when $\theta = \pi/2$ and $\theta = 0$ are very small, i.e., that the anisotropy of interaction is weak. This is mostly due to the fact that the perpendicular and longitudinal responses of (6,5) carbon nanotubes are quite similar, as shown in Fig. 4. The retarded dispersion interaction for $\ell = 4$ nm and $\theta = 0$ is $-0.011\,86\ k_B T/\mathrm{nm}$, while the corresponding value for $\theta = \pi/2$ is $-0.011\,52\ k_B T/\mathrm{nm}$ (3% difference). We show how the retarded interaction changes with angle θ for $\ell = 4$ nm in Fig. 5.
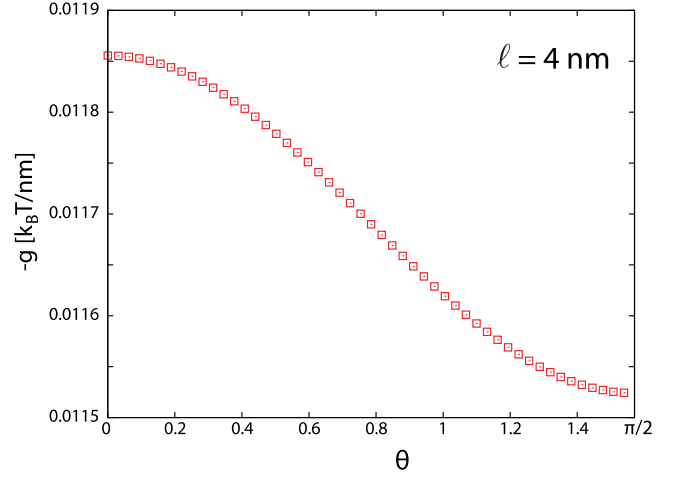

FIG. 5. (Color online) Retarded dispersion interaction between (6,5) SWCNT and a half space made of (6,5) SWCNTs as a function of the angle θ between the longitudinal axes of the two subsystems. The distance between the two subsystems is $\ell = 4$ nm.

IV. EFFECTS OF RETARDATION AND NONMONOTONIC BEHAVIOR OF DISPERSION INTERACTION: DESIGNING A MEDIUM

We want to see whether the formulas derived thus far support a nonmonotonic behavior of dispersion interaction. The nonretarded interaction cannot change its flavor, i.e., it will always be strictly attractive or repulsive, irrespectively of distance ℓ, depending on the properties of the spectra and whether the total sum over Matsubara frequencies is positive or negative.[7] The retarded interaction is different, however. It is known that the retardation effectively restricts sampling of the frequency region, depending on the distance between the objects.[7] For larger distances, the high frequency portion of the spectra is effectively cut off by retardation effects. This is illustrated in Fig. 6 in the example of vdW interaction be-
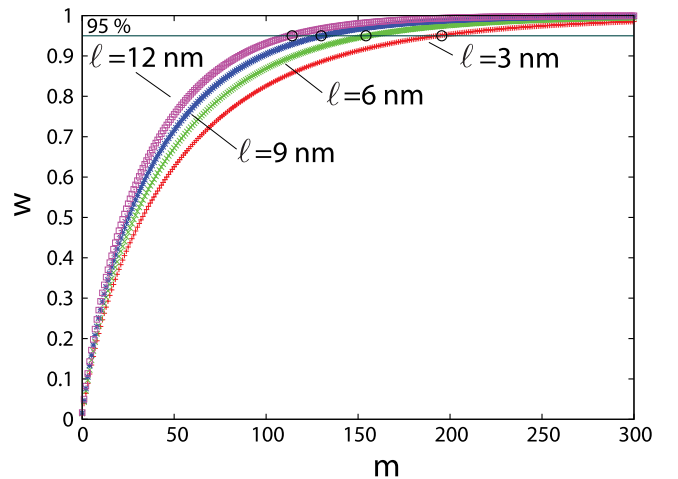

FIG. 6. (Color online) Illustration of the cutoff effect of retardation for a (6,5) carbon nanotube interacting with the gold half space in vacuum—the partial sums are shown for several different separations ℓ between the SWCNT and the half space, as indicated. The *x*-axis is the order of the summation, see Eq. (15).
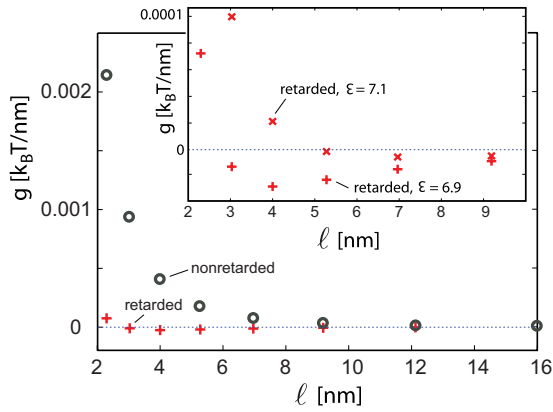
FIG. 7. (Color online) Retarded (crosses) and nonretarded (circles) vdW interactions between a (6,5) CNT and golden half space as a function of distance. The parameters of the medium are $m=17$, $\sigma=2$, and $\mathcal{E}=6.9$. The inset shows how the retarded vdW interaction depends on $\mathcal{E}$ for $\mathcal{E}=6.9$ and $\mathcal{E}=7.1$.
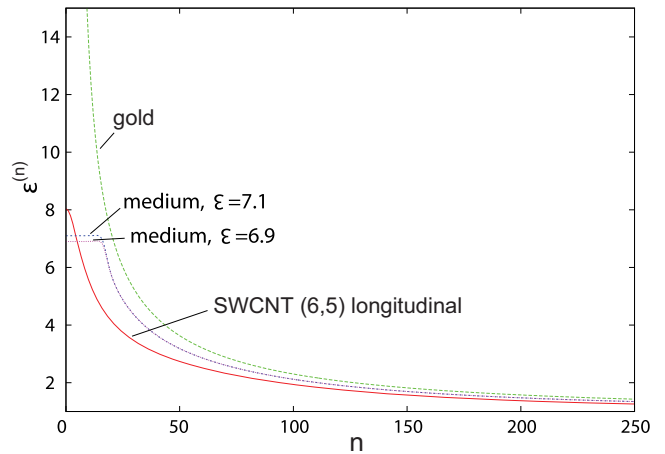

FIG. 8. (Color online) Dielectric responses [gold, SWCNT (6,5), and medium] used in the calculations displayed in Fig. 7. Two different models of the medium, differing only in parameter $\mathcal{E}$, are denoted.

tween a (6,5) carbon nanotube above a golden half space in vacuum. The dielectric response for gold along imaginary axis has been constructed from the absorption data as explained in Ref. 7. The quantity shown on the y-axis is defined as

$$w(m) \equiv \frac{\sum_{n=0}^{m}{}' \int_0^\infty dr \int_0^{2\pi} d\phi \, [e^{-2\ell\rho_3} \mathcal{N}/\mathcal{D}]}{\sum_{n=0}^{\infty}{}' \int_0^\infty dr \int_0^{2\pi} d\phi \, [e^{-2\ell\rho_3} \mathcal{N}/\mathcal{D}]}, \tag{15}$$

see Eq. (4). The cutoff effect of retardation will be more complicated when ϵ_3 also has structure, i.e., when the medium between the half space and the cylinder is not vacuum.

We shall now attempt to *design* the dielectric response of the medium which could produce potentially interesting effects in the vdW interaction. One possible way to do this is to combine two forms of the medium response, $\epsilon_3 = \mathcal{E}$ [vacuumlike, the nonretarded half-space isotropic cylinder ($\epsilon_{2,\perp}^c = \epsilon_{2,\parallel}^c = \epsilon_2^c$) interaction is attractive when $\mathcal{E} < \epsilon_1, \epsilon_2^c$ or $\mathcal{E} > \epsilon_1, \epsilon_2^c$] and $\epsilon_3 = (\epsilon_1 + \epsilon_2^c)/2$.[6]

The expression for the medium dielectric response that we shall use is

$$\epsilon_3^n = [1 - f(n,m,\sigma)]\mathcal{E} + f(n,m,\sigma)\frac{\epsilon_1 + \epsilon_{cyl,\parallel}}{2}, \tag{16}$$

where

$$f(n,m,\sigma) = \frac{1}{2}\left[1 + \tanh\left(\frac{n-m}{\sigma}\right)\right]. \tag{17}$$

Function $f(n,m,\sigma)$ is used as a "switch" between the two functional behaviors of the medium dielectric response, switching at $n=m$ with an effective width of σ. We shall now illustrate the effect of the designed medium on the interaction of a (6,5) SWCNT with golden half space. Figure 7 displays retarded and nonretarded values of dispersion interaction for medium constructed with parameters $m=17.0$, $\sigma=2.0$, and $\mathcal{E}=6.9$ ($\mathcal{E}=7.1$).

This clearly illustrates that the minimum in retarded vdW interaction is possible, but in order to clearly understand its origin, a visual inspection of the dielectric responses is needed, which we show in Fig. 8.

The dielectric response of gold when $n=0$ is huge and off the scale in Fig. 8 ($\epsilon_1^{(0)}=555.9$). Note how small changes in the medium dielectric response induce large changes in the position and magnitude of the vdW minimum (compare Figs. 7 and 8). In fact, the minimum in the retarded vdW interaction is extremely sensitive to details of the medium dielectric response and is easily lost, in our case when $\mathcal{E}$ goes outside interval $\langle 6.5, 7.4 \rangle$, all other parameters being fixed.

The same analysis can be repeated for other materials of the substrate (half space). In Fig. 9 we show the dielectric responses of the half space made of polystyrene (again an optically isotropic material), the longitudinal response of a (6,5) SWCNT, and the medium constructed with $m=18.0$, $\sigma=30.0$, and $\mathcal{E}=8.4$. In this case, due to a large magnitude of parameter σ, the medium dielectric response crosses the
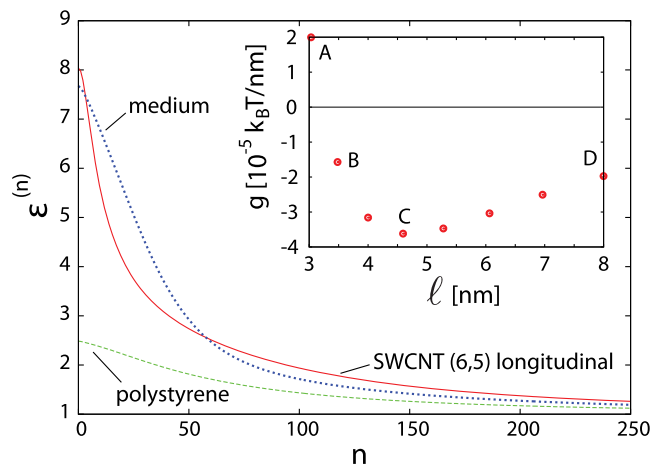

FIG. 9. (Color online) Dielectric responses [polystyrene, SWCNT (6,5), and medium] used in the calculation of the retarded dispersion interaction displayed in the inset of the figure.
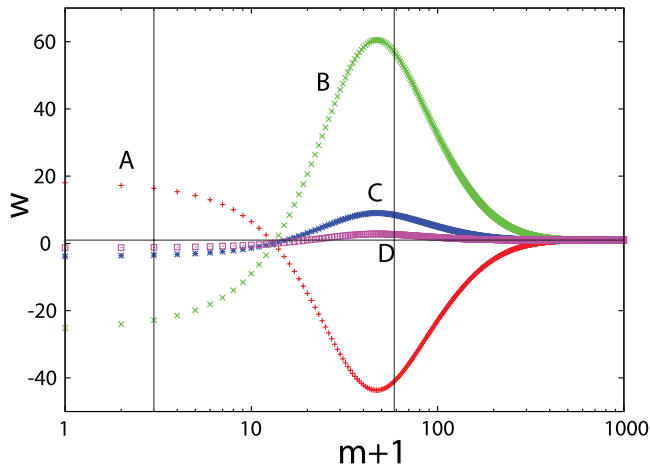
FIG. 10. (Color online) Contributions of different parts of the spectra to the total vdW interaction. A w function defined by Eq. (15) is shown on the y-axis for four different separations between CNT (6,5) and polystyrene: 3.03 nm (a), 3.48 nm (b), 4.59 nm (c), and 8.0 nm (d). The dielectric response of the medium in these calculations is shown in Fig. 9. A thin horizontal line denotes the value of $w=1$ [i.e., the limit $\lim_{m \to \infty} w(m)$]. Two thin vertical lines denote the positions where the medium dielectric response crosses the longitudinal CNT (6,5) response (see Fig. 9). Note that the vdW interaction is repulsive for (a) and attractive for (b)–(d).

SWCNT response twice, close to $n=3$ and $n=58$. So, the contributions to dispersion interaction from different frequency regions are repulsive $(0<n<3)$-attractive $(3<n<58)$-repulsive $(n>58)$ (we should emphasize here that this conclusion is based on simplified expression for *nonretarded* and *isotropic* variant of the dispersion interaction—see, however, Fig. 10). The dispersion interaction calculated with such a medium is shown in the inset of Fig. 9. Note again the appearance of the minimum, still feeble on the thermal energy scale (this depends, however, also on the total length of the carbon nanotube which can be hundreds of microns long[1,5]).

We now examine the contributions of different parts of the spectra to the total sum. This is shown in Fig. 10 for the case of (6,5) SWCNT interacting with polystyrene half space with a medium designed as displayed in Fig. 9. The values of w from Eq. (15) are shown for four different SWCNT-polystyrene distances denoted by (a)–(d), as in the inset of Fig. 9. Note how the total sum is much smaller from the contribution that would be obtained, e.g., by summing only in the infrared and visible regions, this contribution would be about 50 times larger than the total interaction (for ℓ =3.48 nm) and of the wrong sign. This indicates that in order to accurately predict possibly "exotic" effects in dispersion interaction, one needs to know the details of dielectric spectra of all the materials in a huge range of frequencies due to cancellations that may occur in the Matsubara sum (as is the case here).

V. SUMMARY AND CONCLUSIONS

We have derived the expressions for the dispersion interaction between an optically anisotropic semiconducting/insulating cylinder and an anisotropic semi-infinite substrate.

The final formulas account for the effects of retardation and we find that these are relatively small (about 7%) for distances of the order of $\ell \sim 4$ nm. Their effect becomes progressively more important with the separation and contributes about a half of total interaction at $\ell \sim 40$ nm. We have found that the dispersion interaction may show nonmonotonic behavior, changing character from repulsive to attractive at some crossover distance. This effect is, however, very fragile and depends strongly on the details of the medium optical response and its relation to the response of the two subsystems.[15]

The validity of our approach is limited by several conditions based on the observation whether the expansion of the Barash result[11] in terms of the vanishing volume fraction of anisotropic dielectric cylinders, i.e., the Pitaevskii limit, exists or not. It exists first of all if the material has a finite dielectric response for all the frequencies. This condition excludes the metallic SWCNTs from our consideration. The additional condition for the existence of the Pitaevskii limit is that one can disregard the multiple scattering terms[10] in the interaction. This condition stipulates that the radius of the cylinder should be the smallest length in the system and excludes all finite-size effects. Although our approach thus has severe limitations, we are nevertheless convinced of its usefulness since exact calculations for an anisotropic finite cylinder above an anisotropic dielectric surface have been difficult to get.

This article together with Ref. 6 concludes our investigation of the retarded vdW interactions between two anisotropic dielectric cylinders and between an anisotropic dielectric cylinder and a semi-infinite substrate.

[1] R. Saito, G. Dresselhaus, and M. S. Dresselhaus, *Physical Properties of Carbon Nanotubes*, 1st ed. (World Scientific, Singapore, 1998).
[2] R. F. Rajter, R. Podgornik, V. A. Parsegian, R. H. French, and W. Y. Ching, Phys. Rev. B **76**, 045417 (2007).
[3] R. F. Rajter, R. H. French, R. Podgornik, W. Y. Ching, and V. A. Parsegian, J. Appl. Phys. **104**, 053513 (2008).
[4] M. Zheng and E. D. Semke, J. Am. Chem. Soc. **129**, 6084 (2007) (and references therein).
[5] M. J. Bronikowski, Carbon **44**, 2822 (2006).
[6] A. Šiber, R. F. Rajter, R. H. French, W. Y. Ching, V. A. Parsegian, and R. Podgornik, Phys. Rev. B **80**, 165414 (2009).

[7]V. A. Parsegian, *Van der Waals Forces* (Cambridge University Press, Cambridge, 2005).

[8]R. H. French *et al.*, Rev. Mod Phys. (2010) (in press).

[9]L. P. Pitaevskii, Sov. Phys. JETP **10**, 408 (1960).

[10]T. Emig, N. Graham, R. L. Jaffe, and M. Kardar, Phys. Rev. Lett. **99**, 170403 (2007).

[11]Yu. S. Barash, Izv. Vyssh. Uchebn. Zaved., Radiofiz. **21**, 163 (1978); J. N. Munday, D. Iannuzzi, Yu. S. Barash, and F. Capasso, Phys. Rev. A **71**,

042102 (2005); both papers contain a typo that was corrected in Ref. 12.

[12]J. N. Munday, D. Iannuzzi, Yu. Barash, and F. Capasso, Phys. Rev. A **78**, 029906 (2008).

[13]Yu. S. Barash and A. A. Kyasov, Sov. Phys. JETP **68**, 39 (1989).

[14]Wolfram Research, Inc., MATHEMATICA, Version 7.0, Champaign, IL (2008).

[15]M. Elbaum and M. Schick, Phys. Rev. Lett. **66**, 1713 (1991).